Dalton Transactions

Accepted Manuscript

ROYAL SOCIETY OF CHEMISTRY

www.rsc.org/dalton

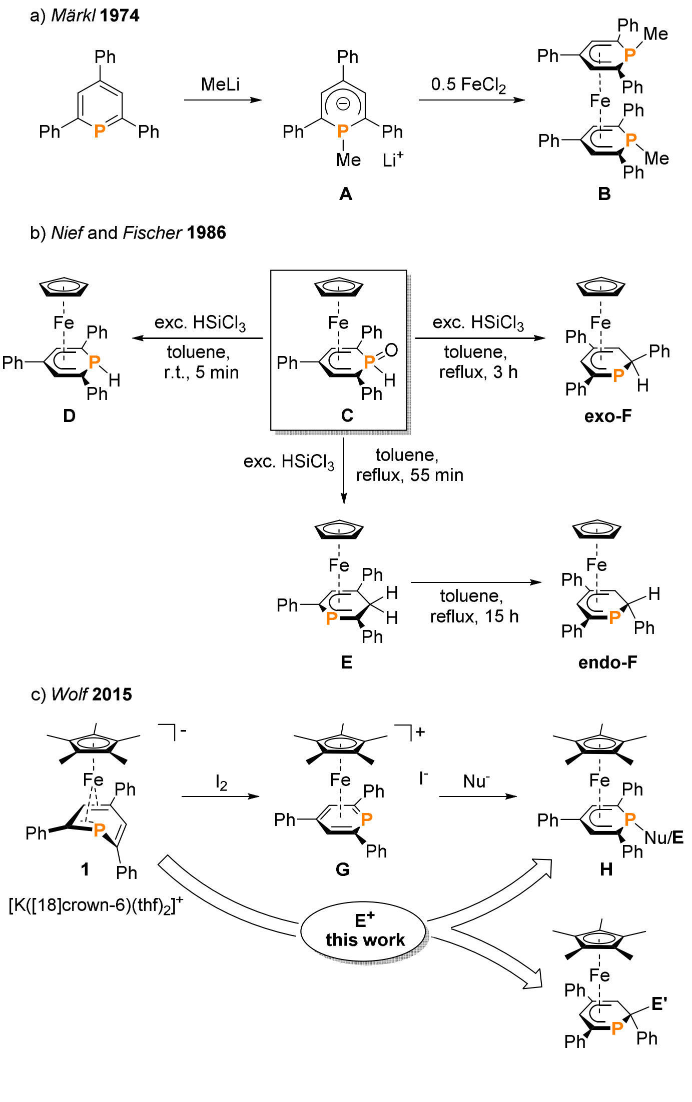

Figure 2 Synthesis of phosphacyclohexadienyl complexes; Nu = H, NMe_2, Cp*;[7] E = H, Me, $SiMe_3$, PPh_2; E' = H, BCat.

To our knowledge, **endo-F** is the only crystallographically characterized example of a 2-R-substituted phosphacyclohexadienyl complex with the C_4P coordination mode so far. Using a different approach, we synthesized η^5-phosphacyclohexadienyl iron complexes of type **H** by oxidizing the anionic pentamethylcyclopentadienyl complex **1** with iodine, followed by the conversion of the resulting cationic complex **G** with nucleopiles (Figure 2c).[7] Nucleophilic attack occurs at the phosphorus atom, giving 1-substituted $\lambda^3\sigma^3$-phosphacyclohexadienyl complexes. While this route can in principle give access to a large family of complexes, a disadvantage is the required two-step reaction sequence. In this paper, we report a new, complementary route to phosphacyclohexadienyl complexes that is based on the *direct* reaction of the anion **1** with electrophiles. The application of this new method resulted in the synthesis and structural characterization of six new phosphacyclohexadienyl complexes **endo-3**, **exo-3**, and **4** – **7**. The formation of 1- phosphacyclohexadienyls (where the substituents are attached to phosphorus) and 2-substituted phosphacyclohexadienyls (where the substituent is connected to an adjacent carbon atom) is observed. Consequently, the molecular structures of the complexes display the C_5 and the C_4P coordination mode, respectively (Figure 1).

Results and discussion

Synthesis of novel phosphacyclohexadienyl complexes

We recently reported that the 1-hydrophosphacyclohexadienyl complex **2** can be synthesized by reacting the cationic phosphinine complex **G** with one equivalent $LiBHEt_3$ (Figure 2c). Assuming that the protonation of the anionic complex **1** might give the same product, **1** was treated with one equivalent of $HCl(OEt_2)$ in THF. The reaction affords a mixture of compounds, including **2** and the new compounds **endo-3** and **exo-3**. The latter are isomers of **2** and display 2-hydrophosphacyclohexadienyl ligands. In the case of **endo-3**, the hydrogen atom in the 2-position of the phosphinine is attached to the metal-coordinated face, causing the phenyl substituent to point to the bottom. The diastereomer **exo-3** formally results from protonation of the phosphinine ring at the remote face to the iron center. Isomers **2**, **endo-3** and **exo-3** are analogous to **D**, **endo-F** and **exo-F** previously prepared by *Nief* and *Fisher* via a completely different route (Figure 2b).[8]

$^{31}P\{^1H\}$ NMR monitoring ([D_8]THF, Figure 3) revealed the signal of **2** (−80 ppm) at −80 °C. Two additional signals at 10 ppm and −64 ppm arise from unknown intermediates, which disappear at higher temperature. The signal of the starting material **1** (−49 ppm) continuously decreased on slow warming to 0 °C, whereas the signal of **2** increased. The signals of the 2-H-substituted species **exo-3** (−162 ppm) and **endo-3** (−137 ppm) were observed in low intensity at −30 °C; their intensity increased significantly at 0 °C, whereas the signal of **2** decreased. An additional signal corresponding to an unidentified species became apparent at −14 ppm at −40 °C. This signal could plausibly arise from a by-product similar to complex **E** (−20.4 ppm)[8] or a decomposition product. The $^{31}P\{^1H\}$ NMR spectrum of the reaction mixture recorded at room temperature displays the signals of **2**, **exo-3**, **endo-3** as well as a few weak singlets of further unidentified species. The signal intensities did not change further after one day. Stirring the raw product mixtures of **2**, **endo-3** and **exo-3** at 50 °C for several days ($^{31}P\{^1H\}$ NMR monitoring) also did not lead to a further change of the integral ratios.

Even though **2** appears to be formed selectively at low temperature, we were not able to isolate it as a pure material from reactions performed at −40 °C. However, **2** slowly converts to **exo-3** upon treatment with $HCl(OEt_2)$ (10 mol%) at room temperature in [D_8]THF. This indicates the rearrangement to be acid-catalysed. Attempts to optimise the reaction gave poorly reproducible product mixtures. Thus, it appears difficult to access 2, exo-3 and endo-3 as pure compounds by protonationg 1 with HCl(OEt2).

The results of the monitoring experiment indicate that the 1-hydrophosphacyclohexadienyl complex **2** is formed as the main kinetic product along with two unidentified species (marked with an asterisk in Figure 3). The 2-hydrophosphacyclohexadienyl

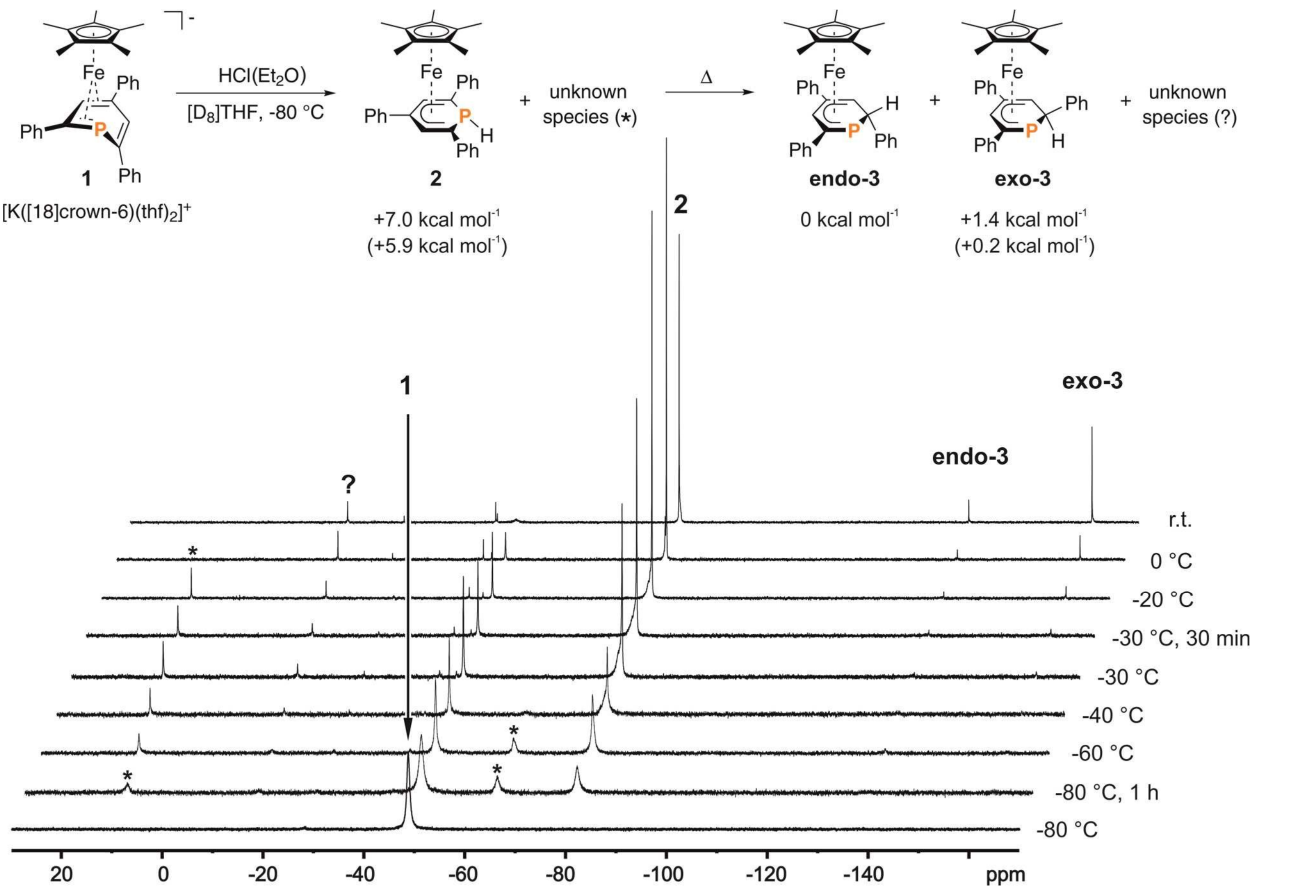

Figure 3 $^{31}P\{^1H\}$ NMR monitoring of the reaction of **1** with HCl(Et$_2$O) in [D$_8$]THF; * and ? designate unknown intermediates or products; the scheme represents the proposed reaction pathway for the protonation of **1**; DFT-calculated (BP86/def2-TZVP level) relative thermal enthalpies (ΔH at 298 K) are given of **2**, **endo-3** and **exo-3**; the relative free enthalpies (ΔG at 298 K) are given in parentheses; see the ESI for details.

complexes **endo-3** and **exo-3** appear to be thermodynamic products that form at higher temperatures. Indeed, gas-phase DFT calculations performed at the BP86/def2-TZVP level (see the experimental section for details) indicate that **endo-3** and **exo-3** are close in energy, while **2** was calculated to be +7.0 kcal mol^{-1} less stable than **endo-3** (Figure 3, see the experimental section for details).

Gratifyingly, the reaction of **1** with one equiv. isopropyl chloride in THF at room temperature (Scheme 1) proceeded cleanly, reproducibly affording a mixture of **endo-3** and **exo-3** in a 65:35 ratio (NMR integration). The formation of **2** as an intermediate was not observed by $^{31}P\{^1H\}$ NMR in this case, which indicates that the reaction proceeds via a different mechanism. Purification by column chromatography gave NMR-spectroscopically pure **exo-3** and **endo-3** after crystallization.

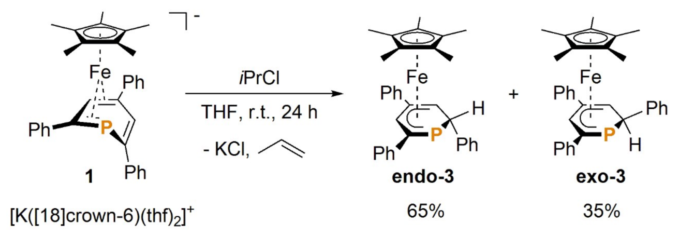

Scheme 1 Preparation of **endo-3** and **exo-3**.

Exo-3 was isolated as orange rods in 25% yield, whereas pure **endo-3** crystallized as orange plates in 41% yield. Both compounds are air-sensitive and dissolve well in *n*-hexane, diethyl ether, toluene and THF.

Complexes **4** – **6** are accessible in a similar fashion in moderate yields by reacting **1** with one equiv. of MeI, Me_3SiCl, and Ph_2PCl (Scheme 2a-c).§ The compounds are deeply coloured crystalline solids that dissolve well in polar and apolar solvents such as *n*-pentane, *n*-hexane, diethyl ether, toluene and THF.

The 2-substituted phosphacyclohexadienyl complex **7** was obtained as bright orange crystals by a similar reaction with one equiv. of chlorocatecholborane (Scheme 2d). Compound **7** is moderately soluble in *n*-pentane and *n*-hexane, but dissolves well in more polar solvents such as diethyl ether, toluene and THF. $^{31}P\{^1H\}$ NMR monitoring ([D$_8$]THF, see ESI, Figure S23) at −100 °C revealed a signal at −26 ppm, which we tentatively assign to the intermediate [Cp*Fe(1-BCat-PC$_5$Ph$_3$H$_2$)] (**7-P**, Scheme 3) containing a direct P−B bond. The signal is broad, therefore the ^{31}P-$^{10/11}B$ coupling constant cannot be precisely determined, but the characteristic 1:1:1:1 quartet structure is clearly visible. The resonance of intermediate **7-B** decreased upon warming and completely disappeared at −40 °C. The signal of **7** simultaneously appeared above −60 °C.

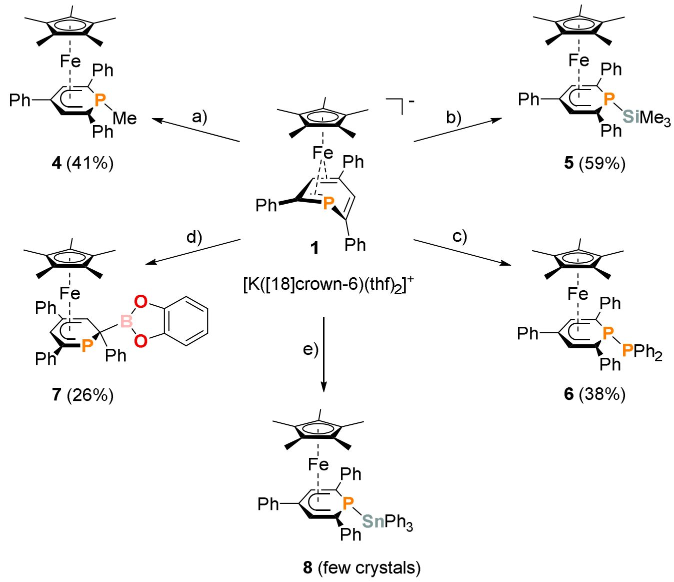

Scheme 2 Synthesis of novel η⁵-phosphacyclohexadienyl complexes **4** – **8**; reagents and by-products: (a) +MeI/−KI, −[18]crown-6; (b) +Me_3SiCl/−KCl, −[18]crown-6; (c) +Ph_2PCl/−KCl, −[18]crown-6; (d) +chlorocatecholborane/−KCl, −[18]crown-6; (e) +Ph_3SnCl/−KCl, −[18]crown-6; isolated yields of the products are given in parentheses.

The $^{31}P\{^1H\}$ NMR spectrum recorded at room temperature shows the presence of **7**, the diphoshinine complex [Cp*$_2$Fe$_2$(μ-{PC$_5$Ph$_3$H$_2$}$_2$)], the hydrophosphinine complex **endo-3** and a small signal for an unidentified by-product (singlet at −50 ppm). The observation of this mixture shows that other processes than

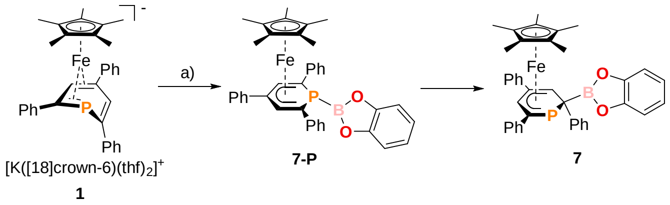

Scheme 3 Presumed formation of 2-subsituted **7** via the 1-substituted intermediate 7-P; reagents and by-products: (a) +chlorocatecholborane/−KCl, −[18]crown-6.

borylation may also occur, explaining the modest isolated yield (26%).

An analogous reaction with Ph_3SnCl in THF produced the P–Sn functionalized complex **8** (Scheme 2e), but the reaction was unselective. According to $^{31}P\{^1H\}$ NMR integration complex **8** is only present in a low amount (26% of the total P content) in the reaction mixture after stirring for 17 h at room temperature. Several attempts to isolate it as a pure compound were not successful due to its low stability. Diphospinine [Cp*Fe(PC$_5$Ph$_3$H$_2$)]$_2$ and hexaphenyldistannane were identified as decomposition products by $^{31}P\{^1H\}$ and $^{119}Sn\{^1H\}$ NMR, suggesting decomposition by a radical pathway.

Crystallographic characterization of exo-3, endo-3, and 4 – 7

Single-crystal X-ray structure determinations of **exo-3, endo-3** and **4** – **7** (Figure 4 and Table 1) revealed η⁵-Cp* and η⁵-phos-

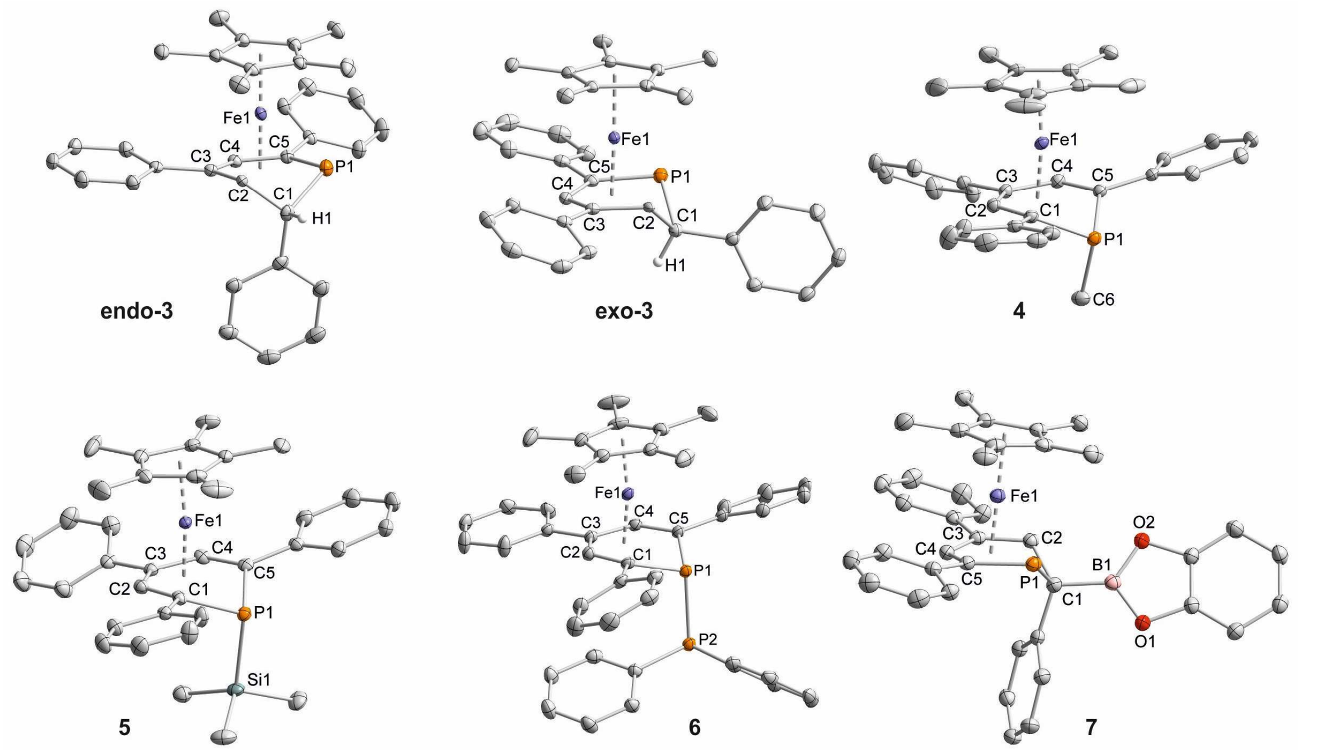

Figure 4 Solid-state molecular structures of complexes **endo-3, exo-3** and **4** – **7**. Ellipsoids are drawn at the 40% probability level; H atoms except H1 in **endo-3** and **exo-3**, and [18]crown-6 in **7** are omitted for clarity, key bond lengths (Å) and angles (°) for **4**: P1–C6 1.853(2), C1–P1–C6 103.94(7), C5–P1–C6 102.72(7); for **5**: P1–Si1 2.270(2), C1–P1–Si1 104.4(1), C5–P1–Si1 106.6(1); for **6**: P1–P2 2.3062(7), C1–P1–P2 107.54(7), C5–P1–P2 105.82(7); for **7**: C1–B1 1.563(2), B1–O1 1.385(2), B1–O2 1.388(2), P1–C1–B1 104.11(1), C2–C1–B1 113.0(1), O1–B1–C1 123.3(1), O2–B1–C1 125.5(1), O1–B1–O2 111.2(1); see Table 1 for additional structural data.

phacyclohexadienyl ligands. As a consequence, the phosphacyclohexadienyl units are not planar. The P atom points away from iron in complexes **4** – **6**, and the heterocycle is folded along the C1–C5 axis. The dihedral angles between the carbocyclic mean plane and the plane defined by C1/P1/C5 (39.4° for **4**, 37.0° for **5**) are close to the values in the related complexes **2** (38.2°) and [Cp*Fe(1-Cp*-$PC_5Ph_3H_2$)] (39.7°) previously reported by us (Figure 2c, *vide supra*).[7] The corresponding fold angle for **6** (27.2°) is over 10° shorter and similar to that of [Cp*Fe(1-NMe_2-$PC_5Ph_3H_2$)] (28.1°, *vide supra*).[7]

Table 1 Selected Bond Lengths (Å) and Angles (°) of the Structures of Compounds **endo-3**, **exo-3** and **4** – **7**.

	endo-3	**exo-3**	**4**	**5**	**6**	**7**
Fe1–P1	2.3125(5)	2.2946(6)	2.8786(4)	2.871(1)	2.7785(5)	2.2783(4)
Fe1–C1	2.881(2)	2.933(2)	2.160(1)	2.168(4)	2.170(2)	2.901(2)
Fe1–C2	2.103(2)	2.133(2)	2.059(1)	2.052(4)	2.048(2)	2.087(2)
Fe1–C3	2.059(1)	2.061(2)	2.091(1)	2.088(4)	2.086(2)	2.061(2)
Fe1–C4	2.090(2)	2.085(2)	2.049(1)	2.050(4)	2.057(2)	2.092(2)
Fe1–C5	2.098(2)	2.096(2)	2.150(1)	2.151(4)	2.161(2)	2.096(2)
Fe1–Cp*(c)[a]	1.700(1)	1.703(1)	1.698(1)	1.699(2)	1.693(1)	1.701(1)
P1–C1	1.851(2)	1.870(2)	1.818(1)	1.828(5)	1.795(2)	1.891(2)
C1–C2	1.521(2)	1.540(3)	1.418(2)	1.404(6)	1.414(3)	1.526(2)
C2–C3	1.459(2)	1.456(3)	1.422(2)	1.435(6)	1.428(3)	1.432(2)
C3–C4	1.433(2)	1.421(3)	1.428(2)	1.430(6)	1.423(3)	1.4272)
C4–C5	1.419(2)	1.427(3)	1.423(2)	1.429(6)	1.414(3)	1.416(2)
P1–C5	1.786(2)	1.792(2)	1.809(1)	1.819(4)	1.801(2)	1.785(2)
P1–C1–C2	98.3(1)	96.0(1)	119.5(1)	120.9(3)	123.6(2)	95.50(9)

a) Cp*(c) = centroid of the cyclopentadienyl ring

In **exo-3**, **endo-3** and **7** the C1 atom adjacent to phosphorus is bent away from the iron center; consequently the six-membered phosphinine ring is folded along the P1–C2 axis. The corresponding plane to plane angles are larger than in **4** – **6** (60.6° for **endo-3**, 63.4° for **exo-3** and 59.7° for **7**). Complexes **endo-3**, **exo-3** and **7** are rare phosphinine-type complexes, which show η^5-coordination through a C_4P-unit. To the best of our knowledge, the sole example comprising the same structural motif is **endo-F** (Figure 2b, *vide supra*).[8]

The C–C distances of the η^5-coordinated C_5 and C_4P-units **exo-3**, **endo-3** and **4** – **7** (Table 1) are in between typical single and double bond distances.[19] Similar bond lengths were observed for the η^6-coordinated phosphinine ring in complex **G**.[7] In addition, it is noteworthy that the C1–C2 distances of **endo-3** (1.521(2) Å), **exo-3** (1.540(3) Å) and **7** (1.526(2) Å) correspond to the value for a normal single bond.[20] The P–C bond lengths in **4** – **6** are typical for single bonds and similar to those in **B** and **H** (Figure 2, *vide supra*).[4,7] The P–C bond lengths are distinct in **endo-3**, **exo-3** and **7**: the P1–C1 distances (1.891(2)–1.851(2) Å) are in the typical range for P–C single bonds,[20] whereas the P1–C5 (1.792(2)–1.785(2) Å) bonds are shorter and close to those found in the η^6-coordinated ring in **G**.[7]

While the P1–Si1 bond length (2.270(2) Å) of **5** is typical for a P–Si single bond,[19] the P1–P2 bond (2.3062(7) Å) of **6** is elongated compared to that in unsymmetrically-substituted diphosphanes such as 9-diphenylphosphanyl-9-phosphabicyclo-[3.3.1]nonane (2.229(1) Å).[21] An analogous observation was made by *Gudat et al*. for *P*-phosphanyldiazaphospholenes, e.g. 2-diphenylphosphanyl-1,3-dimesityldiazaphospholene, which displays a similarly elongated P–P bond (2.334(1) Å).[22]

In **7**, the B1–C1 distance (1.563(2) Å) is in the range of normal boron-carbon single bonds (1.597 Å). The boron centre comprises a trigonal planar environment (angular sum = 360°).[20] It seems noteworthy that *Mathey* and co-workers synthesized related phosphinine borates, e.g. Li[2-BEt_3-PC_5H_4] by reaction of 2-bromophosphinines with two equiv. $LiBHEt_3$.[23] These anionic molecules contain a tetrahedral boron atom in the 2-position; they can be converted into 2-ethylated phosphinines by reaction with iodine. *Braunschweig et al.* prepared a serious of (dimethoxyborylmethyl)dimethylphosphane complexes where a P–C–$B(OMe)_2$ unit of coordinates to chromium or iron via the P atom.[24] An example is the compound [$(FeH(CO)_3(SiPh_3)\{Me_2PCH_2B(OMe)_2\}$]. Different from these σ-coordinated complexes, the phosphacyclohexadienyl ligand of **7** acts as a π-ligand to iron through the planar C_4P-unit. Thus, the phosphorus lone pair remains uncoordinated and should be able to act as a Lewis base. The trivalent boron center might function as a Lewis acid in related complexes with less strongly electron-donating substituents at boron, enabling the formation of a new frustrated Lewis pair type system.

NMR and UV-Vis spectroscopic characterization

Table 2 summarizes ^1H, $^{13}C\{^1H\}$ and $^{31}P\{^1H\}$ NMR data of **endo-3**, **exo-3** and **4** – **7** recorded in $[D_8]$THF. The ^{31}P NMR signals of **exo-3** (−160.7 ppm, $^2J_{PH}$ not detected) and **endo-3** (−136.3 ppm,

Table 2 Characteristic ^{1}H, $^{13}C\{^{1}H\}$ and $^{31}P\{^{1}H\}$ NMR data of complexes **endo-3**, **exo-3** and **4** – **7**; atom labelling according to Figure 3.

	$^{31}P\{^{1}H\}$ NMR	^{1}H NMR			$^{13}C\{^{1}H\}$ NMR	
complex	P1 (ppm)	$C_5(CH_3)_5$ (ppm)	C2–*H*, C4–*H* (ppm)	$^{3}J_{HP}$ (Hz)	*C*1, *C*5 (ppm)	$^{1}J_{C1P}$, $^{1}J_{C5P}$ (Hz)
endo-3	−136.3 (s)	1.36 (s)	2.98 (dd), 7.20–7.24 (m)[a]	2.4	34.7 (d), 95.2 (d)	23.2, 69.9
exo-3	−160.7 (s)	1.30 (s)	2.44 (s), 7.13–7.40 (m)[b]	*n.d.*	31.7 (d), 97.7 (d)	19.7, 67.5
4	−57.4 (s)	1.02 (s)	6.07 (d)	2.6	41.1 (d)	1.1
5	−77.7 (s)	1.02 (s)	6.21 (d)	2.5	29.2 (d)	0.9
6	−38.8 (d)	0.98 (s)	6.02 (d)	2.9	41.0 (dd)	12.5
7	−126.7 (s)	1.34 (s)	3.51 (s), 6.03–6.05 (m)[c]	*n.d.*	*n.d.*, 95.2 (d)	*n.d.*, 74.5

a) overlapping with *meta*–*H* of C5–Ph; *b*) overlapping with Ar–*H* of C1–Ph and *meta*/*para*–*H* of C3–Ph/C5Ph; *c*) overlapping with *ortho*–*H* of C1–Ph; *n.d.* = not detected.

$^{2}J_{PH}$ = 15.2 Hz) are slightly downfield shifted in comparison with those of the cyclopentadienyl analogues **exo-F** (−173.0 ppm) and **endo-F** (−150.1 ppm) synthesised by *Nief* and *Fischer*,[8,25] which otherwise feature similar ^{1}H and ^{13}C NMR shifts of the phosphacyclohexadienyl units as their Cp*-substituted equivalents. Notably, the simple change of the configuration of a carbon atom of the phosphinine ring causes an upfield shift of the ^{31}P NMR doublet of **exo-3** by almost 25 ppm with respect to **endo-3**. The aliphatic hydrogen atom of the phosphinine ring resonate at 2.76 ppm for **endo-3** and at 1.66 ppm for **exo-3**. The spectrum of **exo-3** thus displays a pronounced upfield shift for the exo-hydrogen atom comparable to that observed for the related cyclohexadienyl complex [CpFe(η^5-C_6H_7)].[25]

The spectra of 1-substituted **4** – **6** overall resemble those of related complexes of type **H** (Figure 2c).[7] Characteristic ^{1}H NMR features of **4** and **5** are the doublets at −0.13 ppm ($^{2}J_{PH}$ = 5.5 Hz) for the methyl group of **4** and the Me_3Si group of **5** (−0.41 ppm, $^{3}J_{HP}$ = 3.4 Hz). The $^{31}P\{^{1}H\}$ NMR signal of the trimethylsilyl-substituted complex **5** is upfield shifted by 20.3 ppm compared to the methyl-substituted analogue **4**. Two $^{31}P\{^{1}H\}$ NMR doublets are observed for **6** at 12.8 and −38.8 ppm with a large $^{1}J_{PP}$ coupling constant (293 Hz) in the typical range for a covalent P–P single bond.[26] The signal at 12.8 ppm is assigned to the PPh_2 group, because it splits into a doublet of quintets in the ^{31}P NMR spectrum ($^{3}J_{PH}$ = 6.5 Hz).

Complex **7**, which features a 2-substituted phosphacyclohexadienyl moiety, gives rise to a similar high-field $^{31}P\{^{1}H\}$ NMR singlet (−126.7 ppm) as **endo-3** (−160.7 ppm); the ^{1}H NMR data (Table 2) are also similar in agreement with the similar structures.‡

The UV/vis spectra of **endo-3** – **7** were recorded in *n*-hexane. The spectra of 2-H-substituted **endo-3** and **exo-3** are similar and display a weak shoulder at 450 nm; three stronger bands are found in the UV range (**endo-3** 220, 260 and 320 nm; **exo-3** 230, 275 and 325 nm). The spectrum of the structurally related complex **7** is analogous, showing slightly bathochromically shifted bands at 260, 290sh, 360sh and 460sh nm. The UV/vis spectra of the 1-substituted species **4** – **6** are distinct from those of the aforementioned complexes and feature two visible absorptions each with moderate intensities in the ranges λ_{max} = 550–580 nm and λ_{max} = 480–580 nm, respectively. Similar spectra were observed for other complexes of this type (type **H**, Figure 2c).[7] Previous TD-DFT calculations indicated that these bands predominantly arise from excitations from filled metal-centered MOs into the ligand-based unoccupied MOs (MLCT).[7]

Conclusions

The reaction of the anionic phosphinine complex **1** with diverse electrophiles represents a novel and straightforward synthetic pathway to phosphacyclohexadienyl iron complexes. Protonation of **1** using HCl(OEt_2) initially affords the 1-substituted complex **2** at low temperature, which appears to undergo an acid catalyzed rearrangement and converts to a mixture of isomers, including the 2-H-substituted compounds **endo-3** and **exo-3**. The latter complexes were conveniently isolated in good yields from the reaction of **1** with isopropyl chloride. An analogous 2-substitued complex **7** formed in the reaction with chlorocatecholborane. Similar to the hydrophosphinine complexes, an initial formation of a phosphorus substituted complex followed by a subsequent 1,2-shift of the substituent was observed. Using MeI, Me_3SiCl, Ph_2PhCl and Ph_3SnCl, 1-substituted complexes **4** – **6** and **8** were obtained. Thus, HCl(OEt_2), isopropyl chloride and chlorocatecholborane result in products substituted at the 2-carbon atom, whereas MeI, Me_3SiCl, Ph_3SnCl and Ph_2PhCl provides phosphorus substituted products.

An extensive family of related compounds could become accessible via this route. In addition, the reactivity and possible catalytic activity of the new complexes presented here needs to be examined, where the unusually long P–P bond in **6** and the FLP type motif in **7** will be of particular interest. Investigations in these directions are underway in our laboratory.

Experimental

General Considerations

All experiments were performed under an atmosphere of dry argon, by using standard Schlenk and glovebox techniques. Solvents were purified, dried, and degassed with an MBraun SPS800 solvent purification system. NMR spectra were recorded on Bruker Avance 300 and Avance 400 spectrometers at 300 K and internally referenced to residual solvent resonances. The assignment of the ^{1}H and ^{13}C NMR signals was confirmed by two-dimensional (COSY, HSQC, and HMBC) experiments. Melting points were measured on samples in sealed capillaries on a Stuart SMP10 melting point apparatus. UV/vis spectra were recorded on a Varian Cary 50 spectrometer. Elemental analyses were determined by the analytical department of Regensburg University. The starting material [K([18]crown-6)(thf)$_2$][Cp*Fe(η^4-$PC_5Ph_3H_2$)] (**1**)[7] was prepared according to literature procedures. HCl(Et_2O) solution, methyl iodide, trimethylsilyl chloride, chlorocatecholborane and chlorodiphenylphosphane were purchased from Sigma-Aldrich and TCI and were used as received.

[Cp*Fe(2-*endo*-H-$PC_5Ph_3H_2$)] (endo-3) and [Cp*Fe(2-*exo*-H-$PC_5Ph_3H_2$)] (exo-3). A solution of isopropyl chloride in THF (1.0 mL, c = 0.108 mol·L^{-1}) was added to a dark orange solution of **1** (104 mg, 0.108 mmol) in THF (5 mL). The solution was stirred at room temperature for 24 hours. The resulting dark orange brown mixture was subjected to column chromatography (silica gel, 22 x 1 cm, *n*-hexane/toluene gradient, 100/1 to 5/1). Two bright orange bands were obtained: **exo-3** was eluted first (R_f(*n*-hexane/toluene, 5/1) = 0.42), slightly overlapping with **endo-3**, which followed immediately (R_f(*n*-hexane/toluene, 5/1) = 0.32). Removal of the solvent gave **exo-3** and **endo-3** as pure bright orange solids. Yield of **exo-3**: 14 mg (25%), yield of **endo-3**: 23 mg (41%), total including mixed fractions: 45 mg (80%). X-ray quality crystals formed upon storage of concentrated *n*-hexane solutions at room temperature for three days. Variable elemental analyses were obtained for **exo-3** and **endo-3**. Traces of silica gel can be removed by taking up the product in *n*-hexane, filtration and removal of the solvent.

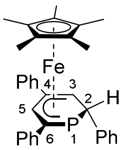

endo-3

endo-3. M.p. 196 °C. UV/vis: (*n*-hexane, λ_{max} / nm, ε_{max} / L·mol^{-1}·cm^{-1}): 220sh (37000), 260 (29600), 320sh (9300), 450sh (670). ^{1}H NMR (400.13 MHz, 300 K, [D$_8$]THF): δ = 1.36 (s, 15H, $C_5(CH_3)_5$), 2.76 (dd, $^2J_{HP}$ = 15.2 Hz, $^3J_{HH}$ = 8.1 Hz, 1H, C^2–*H* of TPP), 2.98 (dd, $^3J_{HP}$ = 2.4 Hz, $^3J_{HH}$ = 8.1 Hz, 1H, C^3–*H* of TPP), 6.77 – 6.81 (m, 3H, C^{2,4,6}–*H* of C^2–Ph), 6.90 – 6.94 (m, 2H, C^{3,5}–*H* of C^2–Ph), 7.16 (t, $^3J_{HH}$ = 7.2 Hz, 1H, C^4–*H* of C^6–Ph), 7.20 – 7.24 (m, 3H, C^{3,5}–*H* of C^6–Ph overlapping with C^5–*H* of TPP), 7.31 (t, $^3J_{HH}$ = 7.3 Hz, 1H, C^4–*H* of C^4–Ph), 7.37 – 7.42 (m, 2H, C^{3,5}–*H* of C^4–Ph), 7.80 (d, 2H, C^{2,6}–*H* of C^6–Ph), 7.93 (d, $^3J_{HH}$ = 7.8 Hz, 2H, C^{2,6}–*H* of C^4–Ph). ^{13}C{^{1}H} NMR (100.61 MHz, 300 K, [D$_8$]THF): δ = 10.0 (d, $^3J_{CP}$ = 3.4 Hz, $C_5(CH_3)_5$), 26.3 (s, *C*^{3}–H of TPP), 34.7 (d, $^1J_{CP}$ = 23.2 Hz, *C*^{2} of TPP), 87.9 (s, $C_5(CH_3)_5$), 88.8 (d, $^2J_{CP}$ = 7.9 Hz, *C*^{5}–H of TPP), 91.8 (s, *C*^{4} of TPP), 95.2 (d, $^1J_{CP}$ = 69.9 Hz, *C*^{6} of TPP), 125.2 (s, *C*^{4}–H of C^2–Ph), 126.3 (d, $^3J_{CP}$ = 3.5 Hz, *C*^{2}–H of C^2–Ph), 127.1 (d, $^5J_{CP}$ = 1.1 Hz, *C*^{4}–H of C^6–Ph), 127.7 (s, *C*^{4}–H of C^4–Ph), 127.5 (s, *C*^{2,6}–H of C^4–Ph), 127.9 (s, *C*^{2,6}–H of C^4–Ph), 128.1 (s, *C*^{3,5}–H of C^2–Ph), 128.6 (d, $^4J_{CP}$ = 1.0 Hz, *C*^{3,5}–H of C^6–Ph), 129.0 (s, *C*^{3,5}–H of C^4–Ph), 141.8 (s, *C*^{1} of *C*^{4}–Ph), 143.8 (d, $^2J_{CP}$ = 17.8 Hz, *C*^{1} of *C*^{6}–Ph), 147.1 (d, $^2J_{CP}$ = 1.8 Hz, *C*^{1} of *C*^{2}–Ph). ^{31}P{^{1}H} NMR (161.98 MHz, 300 K, [D$_8$]THF): δ = −136.3 (s). ^{31}P NMR (161.98 MHz, 300 K, [D$_8$]THF): δ = −136.3 (d, $^2J_{PH}$ = 15.3 Hz). Elemental analysis calcd. for $C_{33}H_{33}FeP$ (Mw = 516.45 g·mol^{-1}) C 76.75, H 6.44; found C 76.11, H 6.55.

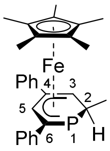

exo-3

exo-3. M.p. 177 °C. UV/vis: (*n*-hexane, λ_{max} / nm, ε_{max} / L·mol^{-1}·cm^{-1}): 230sh (72000), 275 (59000), 325sh (17000), 450sh (1100). ^{1}H NMR (400.13 MHz, 300 K, [D$_8$]THF): δ = 1.30 (s, 15H, $C_5(CH_3)_5$), 1.66 (s br, 1H, C^2–*H* of TPP), 2.44 (s br, 1H, C^3–*H* of TPP), 7.13 – 7.40 (overlapping m, 12H, Ar–*H* of C^2–Ph + C^5–*H* of TPP + C^{3,4,5}–*H* of C^4–Ph + C^{3,4,5}–*H* of C^6–Ph), 7.86 (d, $^3J_{HH}$ = 7.9 Hz, 2H, C^{2,6}–*H* of C^4–Ph), 7.90 (d, $^3J_{HH}$ = 7.9 Hz, 2H, C^{2,6}–*H* of C^6–Ph). ^{13}C{^{1}H} NMR (100.61 MHz, 300 K, [D$_8$]THF): δ = 9.9 (d, $^3J_{CP}$ = 2.8 Hz, $C_5(CH_3)_5$), 21.4 (d, $^2J_{CP}$ = 5.1 Hz, *C*^{3}–H of TPP), 31.7 (d, $^1J_{CP}$ = 19.7 Hz, *C*^{2} of TPP), 86.9 (d, $^2J_{CP}$ = 7.3 Hz, *C*^{5}–H of TPP), 88.1 (s, $C_5(CH_3)_5$), 92.3 (d, $^3J_{CP}$ = 1.8 Hz, *C*^{4} of TPP), 97.7 (d, $^1J_{CP}$ = 67.5 Hz, *C*^{6} of TPP), 125.9, 127.2, 127.3, 127.4, 127.5, 127.6, 127.7, 128.7, 128.9, 129.0 (*C*^{2,3,4,5,6} of C^2–Ph, *C*^{2,3,4,5,6} of *C*^{4}–Ph *C*^{2,3,4,5,6} of *C*^{6}–Ph), 140.8 (s, *C*^{1} of *C*^{4}–Ph), 143.6 (d, $^2J_{CP}$ = 16.7 Hz, *C*^{1} of *C*^{6}–Ph), 145.9 (d, $^2J_{CP}$ = 12.9 Hz, *C*^{1} of *C*^{2}–Ph). ^{31}P{^{1}H} NMR (161.98 MHz, 300 K, [D$_8$]THF): δ = −160.7 (s). ^{31}P NMR (161.98 MHz, 300 K, [D$_8$]THF): δ = −160.7 (s br). Elemental analysis calcd. for $C_{33}H_{33}FeP$ (Mw = 516.45 g·mol^{-1}) C 76.75, H 6.44; found C 77.15, H 6.50.

[Cp*Fe(1-Me-$PC_5Ph_3H_2$)] (4). A solution of methyl iodide in THF (1 mL, c = 0.106 mol·L^{-1}) was added to a dark orange solution of **1** (102 mg, 0.106 mmol) in THF (5 mL) at room temperature. The reaction mixture turned burgundy red immediately, and was stirred for four hours at room temperature. After removing the solvent in *vacuo*, the remaining dark red residue was extracted with *n*-hexane (10 x 1 mL). The burgundy red extracts were combined and the solution was concentrated to 5 mL. Dark red crystals of **4** formed during storage at −30 °C for three days. Yield: 23 mg (41%). M.p. 239 °C. UV/vis: (*n*-hexane, λ_{max} / nm, ε_{max} / L·mol^{-1}·cm^{-1}): 380sh (3150), 480 (1440), 550 (1000). ^{1}H NMR (400.13 MHz, 300 K, [D$_8$]THF): δ = −0.13 (d, $^2J_{HP}$ = 5.5 Hz, 3H, P-C*H*$_3$), 1.02 (s, 15H, $C_5(CH_3)_5$), 6.07 (d, $^3J_{HP}$ = 2.6 Hz, 2H, C^{3,5}–*H* of TPP), 7.12 (t, $^3J_{HH}$ = 7.3 Hz, 2H, C^4–*H* of C^{2,6}–Ph), 7.27 – 7.31 (m, 4H, C^{3,5}–*H* of C^{2,6}–Ph), 7.46 (t, $^3J_{HH}$ = 7.3 Hz, 1H, C^4–*H* of C^4–Ph), 7.54 – 7.58 (m, 2H, C^{3,5}–*H* of C^4–Ph), 8.11 – 8.13 (m, 4H, C^{2,6}–*H* of C^{2,6}–Ph), 8.32 (d, $^3J_{HH}$ = 7.7 Hz, 2H, C^{2,6}–*H* of C^4–Ph). ^{13}C{^{1}H} NMR (100.61 MHz, 300 K, [D$_8$]THF): δ = 8.9 (s, $C_5(CH_3)_5$), 18.2 (d, $^1J_{CP}$ = 39.0 Hz, P–*C*H$_3$), 41.1 (d, $^1J_{CP}$ = 1.1 Hz, *C*^{2,6} of TPP), 79.1 (d, $^2J_{CP}$ = 7.3 Hz, *C*^{3,5}–H of TPP), 85.3 (s, $C_5(CH_3)_5$), 95.9 (d, $^3J_{CP}$ = 2.4 Hz, *C*^{4} of TPP), 124.7 (d, $^5J_{CP}$ = 2.8 Hz, *C*^{4}–H of C^{2,6}–Ph), 128.1 (*C*^{4}–H of C^4–Ph overlapping with *C*^{2,6}–H of C^4–Ph), 128.7 (s, *C*^{3,5}–H of C^{2,6}–Ph), 128.8 (d, $^3J_{CP}$ = 19.5 Hz, *C*^{2,6}–H of C^{2,6}–Ph), 129.4 (s, *C*^{3,5}–H of C^4–Ph), 141.6 (s, *C*^{1} of *C*^{4}–Ph), 145.5 (d, $^2J_{CP}$ = 25.2 Hz, *C*^{1} of *C*^{2,6}–Ph). ^{31}P{^{1}H} NMR (161.98 MHz, 300 K, [D$_8$]THF): δ = −57.4 (s). ^{31}P NMR (161.98 MHz, 300 K, [D$_8$]THF): δ = −57.4 (s, br). Elemental analysis calcd. for $C_{34}H_{35}FeP$ (Mw = 530.47 g·mol^{-1}) C 76.98, H 6.65; found C 77.22, H 6.40.

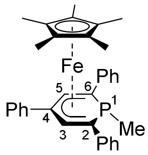

4

[Cp*Fe(1-Me$_3$Si-PC$_5$Ph$_3$H$_2$)] (5). A solution of trimethylsilyl chloride in toluene (0.9 mL, c = 0.152 mol·L^{-1}) was added to a dark orange solution of **1** (132 mg, 0.137 mmol) in THF (7 mL) and stirred at room temperature for 16 h. The resulting dark greenish brown mixture was dried in *vacuo*, and the residue was extracted with *n*-pentane (16 x 0.5 mL). The fractions were combined and dried in *vacuo*. [18]crown-6 was sublimed at 60 °C and < 1.0 · 10^{-3} mbar. The remaining residue was dissolved in *n*-hexane (8 mL). The greenish black solution was filtered and concentrated to 5 mL. **5** was isolated as dark green to black crystals after storage at −30 °C for three days. Yield: 48 mg (59%). M.p. 213 °C. UV/vis: (*n*-hexane, λ_{max} / nm, ε_{max} / L·mol^{-1}·cm^{-1}): 250 (36300), 300 (26000), 500 (2300), 580 (2100). ^{1}H NMR (400.13 MHz, 300 K, [D$_8$]THF): δ = −0.41 (d, $^3J_{PH}$ = 3.4 Hz, 9H, P−Si(C*H*$_3$)$_3$), 1.02 (s, 15H, C$_5$(C*H*$_3$)$_5$), 6.21 (d, $^3J_{PH}$ = 2.5 Hz, 2H, C^{3,5}−*H* of TPP), 7.10 (t, $^3J_{HH}$ = 7.2 Hz, 2H, C^4−*H* of C^{2,6}−Ph), 7.22 − 7.27 (m, 4H, C^{3,5}−*H* of C^{2,6}−Ph), 7.47 (t, $^3J_{HH}$ = 7.3 Hz, 1H, C^4−*H* of C^4−Ph), 7.56 − 7.60 (m, 2H, C^{3,5}−*H* of C^4−Ph), 8.08 − 8.11 (m, 4H, C^{2,6}−*H* of C^{2,6}−Ph), 8.34 (d, $^3J_{HH}$ = 7.8 Hz, 2H, C^{2,6}−*H* of C^4−Ph). ^{13}C{^{1}H} NMR (100.61 MHz, 300 K, [D$_8$]THF): δ = −0.9 (d, $^2J_{CP}$ = 8.5 Hz, P−Si(*C*H$_3$)$_3$), 8.8 (s, C$_5$(*C*H$_3$)$_5$), 29.2 (d, $^1J_{CP}$ = 0.9 Hz, *C*^{2,6} of TPP), 82.2 (d, $^2J_{CP}$ = 8.3 Hz, *C*^{3,5}−H of TPP), 85.7 (s, *C*$_5$(CH$_3$)$_5$), 97.9 (d, $^3J_{CP}$ = 1.2 Hz, *C*^{4} of TPP), 124.6 (d, $^5J_{CP}$ = 3.1 Hz, *C*^{4}−H of C^{2,6}−Ph), 127.9 (s, *C*^{4}−H of C^4−Ph), 128.3 (s, *C*^{2,6}−H of C^4−Ph), 128.7 (s, *C*^{3,5}−H of C^{2,6}−Ph and d, $^3J_{CP}$ =19.4 Hz, *C*^{2,6}−H of C^{2,6}−Ph), 129.5 (s, *C*^{3,5}−H of C^4−Ph), 142.5 (s, *C*^{1} of *C*^{4}−Ph), 146.5 (d, $^2J_{CP}$ = 24.2 Hz, *C*^{1} of *C*^{2,6}−Ph). ^{29}Si DEPT NMR (79.49 MHz, 300 K, [D$_8$]THF): δ = −3.3 (d, $^1J_{SiP}$ = 62.4 Hz). ^{31}P{^{1}H} NMR (161.98 MHz, 300 K, [D$_8$]THF): δ = −77.7 (s, ^{29}Si-satellites: $^1J_{PSi}$ = 62.1 Hz). ^{31}P NMR (161.98 MHz, 300 K, [D$_8$]THF): δ = −77.7 (s, br). Elemental analysis calcd. for $C_{36}H_{41}FePSi$ (Mw = 588.63 g·mol^{-1}) C 73.46, H 7.02; found C 73.81, H 6.97.

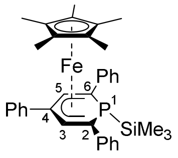

5

[Cp*Fe(1-PPh$_2$-PC$_5$Ph$_3$H$_2$)] (6). A solution of chlorodiphenylphosphane (35 mg, 0.159 mmol) in THF (5 mL) at −95 °C was added dropwise to a dark orange solution of **1** (150 mg, 0.156 mmol) in THF (10 mL) at −95 °C. The reaction mixture turned deep red to violet and was slowly warmed to room temperature. The solvent was removed in vacuo after stirring at room temperature for 16 h. The remaining residue was extracted with *n*-pentane (8 x 1 mL). The extracted fractions were combined and concentrated to 4 mL. **6** was isolated as dark violet crystals after storage at −30 °C for three days. Yield: 48 mg (38%). M.p. 192 °C. UV/vis: (*n*-hexane, λ_{max} / nm, ε_{max} / L·mol^{-1}·cm^{-1}): 240sh (42000), 295 (30800), 485 (2400), 550 (1900). ^{1}H NMR (400.13 MHz, 300 K, [D$_8$]THF): δ = 0.98 (s, 15H, C$_5$(C*H*$_3$)$_5$), 6.02 (d, $^3J_{HP}$ = 2.9 Hz, 2H, C^3−*H* of TPP), 6.84 − 6.93 (m, 6H, C^{3,4,5}−*H* of PPh$_2$), 6.96 − 7.00 (m, 4H, C^{2,6}−*H* of PPh$_2$), 7.10 (t, $^3J_{HH}$ = 7.2 Hz, 2H, C^4−*H* of C^{2,6}−Ph), 7.21 − 7.25 (m, 4H, C^{3,5}−*H* of C^{2,6}−Ph), 7.47 (t, $^3J_{HH}$ = 7.2 Hz, 1H, C^4−*H* of C^4−Ph), 7.52 − 7.56 (m, 2H, C^{3,5}−*H* of C^4−Ph), 7.99 − 8.02 (m, 4H, C^{2,6}−*H* of C^{2,6}−Ph), 8.13 (d, $^3J_{HH}$ = 7.8 Hz, 2H, C^{2,6}−*H* of C^4−Ph). ^{13}C{^{1}H} NMR (100.61 MHz, 300 K, [D$_8$]THF): δ = 8.79 (s, C$_5$(*C*H$_3$)$_5$), 41.0 (dd, $^1J_{CP}$ = 12.5 Hz, $^2J_{CP}$ = 10.6 Hz, *C*^{2,6} of TPP), 80.9 (dd, $^2J_{CP}$ = 12.6 Hz, $^3J_{CP}$ = 10.5 Hz, *C*^{3}−H of TPP), 85.8 (s, *C*$_5$(CH$_3$)$_5$), 97.3 (d, $^3J_{CP}$ = 2.2 Hz, *C*^{4} of TPP), 125.0 (d, $^5J_{CP}$ = 3.3 Hz, *C*^{4}−H of C^{2,6}−Ph), 127.4 (s, *C*^{4}−H of PPh$_2$), 128.0 (d, $^3J_{CP}$ = 6.0 Hz, *C*^{3,5} of PPh$_2$), 128.1 (s, *C*^{4}−H of C^4−Ph), 128.4 (s, *C*^{2,6}−H of C^4−Ph), 128.6 (s, *C*^{3,5}−H of C^{2,6}−Ph), 129.1 (s, *C*^{3,5}−H of C^4−Ph), 129.2 (d, $^3J_{CP}$ = 18.1 Hz, *C*^{2}−H of C^{2,6}−Ph), 134.7 (dd, $^2J_{CP}$ = 17.2 Hz, $^3J_{CP}$ = 4.1 Hz, *C*^{2,6}−H of PPh$_2$), 138.7 (dd, $^1J_{CP}$ = 25.5 Hz, $^2J_{CP}$ = 6.9 Hz, *C*^{1} of PPh$_2$), 141.0 (s, *C*^{1} of *C*^{4}−Ph), 144.9 (d, $^2J_{CP}$ = 24.5 Hz, *C*^{1} of *C*^{2,6}−Ph). ^{31}P{^{1}H} NMR (161.98 MHz, 300 K, [D$_8$]THF): δ = 12.8 (d, $^1J_{PP}$ = 293 Hz, *P*Ph$_2$), −38.8 (d, $^1J_{PP}$ = 293 Hz, *P* of TPP). ^{31}P NMR (161.98 MHz, 300 K, [D$_8$]THF): δ = 12.8 (dquint, $^1J_{PP}$ = 293 Hz, $^3J_{PH}$ = 6.5 Hz, *P*Ph$_2$), −38.8 (d, $^1J_{PP}$ = 293 Hz, *P* of TPP). Elemental analysis calcd. for $C_{45}H_{42}FeP_2$ (Mw = 700.62 g·mol^{-1}) C 77.14, H 6.04; found C 77.55, H 6.36.

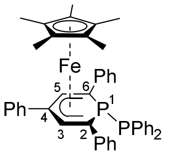

6

[Cp*Fe(2-BCat-PC$_5$Ph$_3$H$_2$)] (7). A solution of chlorocatecholborane (24 mg, 0.155 mmol) in THF (5 mL) was added to a dark orange solution of **1** (150 mg, 0.156 mmol) in THF (10 mL) at −35 °C. The mixture was stirred and warmed to room temperature overnight. All volatiles were removed in *vacuo* and the dark orange-green residue was washed with *n*-hexane (5 x 1 mL) and extracted with diethyl ether (10 x 0.5 mL). The deep orange diethyl ether fractions were combined and the major impurities including [18]crown-6 were crystallized by storage at room temperature for five days. The deep orange mother liquor was decanted and concentrated to 3 mL. Deep orange crystals of **7** formed during storage at room temperature for two days. Yield: 25 mg (25%). M.p. 196 °C (decomposition to a dark green solid). UV/vis: (*n*-hexane, λ_{max} / nm, ε_{max} / L·mol^{-1}·cm^{-1}): 260 (15000), 290sh (10000), 360sh (1700), 460sh (300). ^{1}H NMR (400.13 MHz, 300 K, [D$_8$]THF): δ = 1.34 (s, 15H, C$_5$(C*H*$_3$)$_5$), 3.51 (s, 1H, C^3−*H* of TPP), 6.68 − 6.72 (m, 1H, C^4−*H* of C^2−Ph), 6.89 − 6.91 (m, 2H, C^{3,5}−*H* of C^2−Ph), 6.03 − 6.05 (overlapping m, 3H, C^{2,6}−*H* of C^2−Ph overlapping with C^5−*H* of TPP), 7.07 − 7.11 (m, 2H, C^{2,5}−*H* of catecholboryl), 7.17 − 7.21 (m, 1H, C^4−*H* of C^6−Ph), 7.23 − 7.26 (m, 2H, C^{3,5}−*H* of C^6−Ph), 7.28 − 7.30 (m, 2H, C^{3,4}−*H* of catecholboryl), 7.32 − 7.36 (m, 1H, C^4−*H* of C^4−Ph), 7.44 − 7.48 (m, 2H, C^{3,5}−*H* of C^4−Ph), 7.85 (d, $^3J_{HH}$ = 7.9 Hz, 2H, C^{2,6}−*H* of C^6−Ph), 8.04 (d, $^3J_{HH}$ = 7.9 Hz, 2H, C^{2,6}−*H* of C^4−Ph). ^{13}C{^{1}H} NMR (100.61 MHz, 300 K, [D$_8$]THF): δ = 9.7 (d, $^3J_{CP}$ = 3.2 Hz, C$_5$(*C*H$_3$)$_5$), 26.1 (s, *C*^{3}−H of TPP), 88.4 (s, *C*$_5$(CH$_3$)$_5$), 88.6 (d, $^2J_{CP}$ = 7.3 Hz, *C*^{5}−H of TPP), 90.9 (s, *C*^{4} of TPP), 95.2 (d, $^1J_{CP}$ = 74.5 Hz, *C*^{6} of TPP), 112.9 (s, *C*^{3,4}−H of catecholboryl), 123.3 (s, *C*^{2,5}−H of catecholboryl), 124.3 (s, *C*^{4}−H of C^2−Ph), 127.3 (s, *C*^{2,6}−H of C^4−Ph overlapping with *C*^{4} of *C*^{6}−Ph), 127.4 (d, $^3J_{CP}$ = 4.6 Hz, *C*^{2,6} of *C*^{2}−Ph), 127.6 (s, *C*^{4}−H of C^4−Ph), 127.7 (s, *C*^{3,5}−H of C^2−Ph), 127.9 (d, $^3J_{CP}$ = 15.0 Hz, *C*^{2,6} of *C*^{6}−Ph), 128.7 (s, *C*^{3,5}−H of C^6−Ph), 129.2 (s, *C*^{3,5}−H of C^4−Ph), 141.6 (s, *C*^{1} of C^4−Ph),143.5 (d, $^2J_{CP}$ = 18.0 Hz, *C*^{1} of *C*^{6}−Ph), 147.8 (s, *C*^{1} of C^2−Ph), 149.5 (s, *C*^{1,6} of catecholboryl), the signal for *C*^{2} of TPP was not observed. ^{11}B{^{1}H} NMR (128.38 MHz, 300 K, [D$_8$]THF): δ = 34.3 (s br). ^{11}B

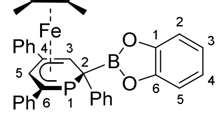

7

NMR (128.38 MHz, 300 K, $[D_8]$THF): δ = 34.3 (s br). $^{31}P\{^1H\}$ NMR (161.98 MHz, 300 K, $[D_8]$THF): δ = −126.7 (s). ^{31}P NMR (161.98 MHz, 300 K, $[D_8]$THF): δ = −126.7 (s br). Elemental analysis calcd. for $C_{39}H_{36}BFeO_2P$ (Mw = 634.34 g·mol^{-1}) C 73.84, H 5.72; found C 73.45, H 5.73.

X-ray Crystallography

Crystals of **endo-3**, **exo-3**, **4**, **5**, and **8** suitable for X-ray diffraction were obtained from *n*-hexane. Crystals of **6** were obtained from diethyl ether. X-ray quality crystals of **7** were obtained from concentrated diethyl ether solutions of the crude reaction mixture resulting in crystallization along with half a molecule of [18]crown-6. The single crystal X-ray diffraction data were recorded on an Agilent Technologies Gemini Ultra R diffractometer (**exo-3** and **5**) and an Agilent Technologies SuperNova (**endo-3**, **4**, and **6** – **8**) with Cu K_α radiation (λ = 1.54184 Å). Semi-empirical multi-scan absorption corrections[27] and analytical ones[28] were applied to the data. The structures were solved with SHELXT[29] and least-square refinements on F^2 were carried out with SHELXL.[29]
CCDC 1448678−1448684 contain the supplementary crystallographic data for this paper. These data can be obtained free of charge from The Cambridge Crystallographic Data Centre via www.ccdc.cam.ac.uk/data_request/cif.

DFT calculations

The calculations on **2**, **endo-3** and **exo-3** were performed using the ORCA program package (version 3.0.2).[31] The BP86 density functional and the Ahlrichs def2-TZVP basis set were employed for all atoms.[32–36] The RI approximation was used.[37,38] The Ahlrichs Coulomb fitting basis for the TZVP basis for all atoms (TZV/J) and the atom-pair-wise dispersion correction to the DFT energy with Becke-Johnson damping (d3bj) were applied.[39,40] The nature of the stationary points was verified by numerical frequency analysis.

Acknowledgements

Funding by the Deutsche Forschungsgemeinschaft is gratefully acknowledged.

Notes and references

§The synthesis of **6** needs to be performed at −95 °C by slow addition of Ph_2PCl to a solution of complex **1**. In this case, **6** was isolated in 38% yield. Addition of Ph_2PCl at room temperature led to an almost quantitative formation of tetraphenyldiphosphane and the dimeric complex $[Cp^*_2Fe_2(\mu\text{-}\{PC_5Ph_3H_2\}_2)]$.[7,41]
‡The $^{13}C\{^1H\}$ NMR resonance for sp^3-hybridized carbon atom of **7** attached to phosphorus and boron was not observed. Coupling in the ^{31}P–^{13}C–$^{10/11}B$ spin system and the quadrupole relaxation mechanism of the ^{11}B nucleus presumably lead to substantial broadening of this signal.[42]

1 C. Müller, L. E. E. Broeckx, I. de Krom and J. J. M. Weemers, *Eur. J. Inorg. Chem.*, 2013, **2013**, 187–202.
2 M. Bruce, G. Meissner, M. Weber, J. Wiecko and C. Müller, *Eur. J. Inorg. Chem.*, 2014, **2014**, 1719–1726.
3 G. Märkl and C. Martin, *Angew. Chem.*, 1974, **86**, 445–446.
4 G. Baum and W. Massa, *Organometallics*, 1985, **4**, 1572–1574.
5 A. Moores, N. Mézailles, L. Ricard and P. Le Floch, *Organometallics*, 2005, **24**, 508–513.
6 A. Moores, L. Ricard, P. Le Floch and N. Mézailles, *Organometallics*, 2003, **22**, 1960–1966.
7 B. Rezaei Rad, U. Chakraborty, B. Mühldorf, J. A. W. Sklorz, M. Bodensteiner, C. Müller and R. Wolf, *Organometallics*, 2015, **34**, 622–635.
8 F. Nief and J. Fischer, *Organometallics*, 1986, **5**, 877–883.
9 M. Doux, N. Mézailles, L. Ricard and P. Le Floch, *Organometallics*, 2003, **22**, 4624–4626.
10 H. Lehmkuhl, J. Elsäßer, R. Benn, B. Gabor, A. Rufińska, R. Goddard, C. Krüger, Z. Naturforsch., 1985, **40b**, 171–181.
11 B. Nuber and M. L. Ziegler, *Acta Crystallogr. C*, 1987, **43**, 59–61.
12 M. Doux, L. Ricard, P. Le Floch and Y. Jean, *Organometallics*, 2005, **24**, 1608–1613.
13 T. Arliguie, M. Doux, N. Mézailles, P. Thuéry, P. Le Floch and M. Ephritikhine, *Inorg. Chem.*, 2006, **45**, 9907–9913.
14 M. Doux, P. Thuéry, M. Blug, L. Ricard, P. Le Floch, T. Arliguie and N. Mézailles, *Organometallics*, 2007, **26**, 5643–5653.
15 T. Arliguie, M. Blug, P. Le Floch, N. Mézailles, P. Thuéry and M. Ephritikhine, *Organometallics*, 2008, **27**, 4158–4165.
16 T. Arliguie, P. Thuéry, P. L. Floch, N. Mézailles and M. Ephritikhine, *Polyhedron*, 2009, **28**, 1578–1582.
17 A. Moores, N. Mézailles, L. Ricard, Y. Jean and P. le Floch, *Organometallics*, 2004, **23**, 2870–2875.
18 H. Lehmkuhl, R. Paul, C. Krüger, Y.-H. Tsay, R. Benn and R. Mynott, *Liebigs Ann. Chem.*, 1981, 1147–1161.
19 P. Pyykkö and M. Atsumi, *Chem. – Eur. J.*, 2009, **15**, 12770–12779.
20 P. Pyykkö and M. Atsumi, *Chem. – Eur. J.*, 2009, **15**, 186–197.
21 D. L. Dodds, J. Floure, M. Garland, M. F. Haddow, T. R. Leonard, C. L. McMullin, A. G. Orpen and P. G. Pringle, *Dalton Trans.*, 2011, **40**, 7137–7146.
22 S. Burck, D. Gudat and M. Nieger, *Angew. Chem.*, 2004, **116**, 4905–4908.
23 D. Carmichael, P. L. Floch, H. G. Trauner and F. Mathey, *Chem. Commun.*, 1996, 971.
24 H. Braunschweig, R. Dirk and B. Ganter, *J. Organomet. Chem.*, 1997, **545–546**, 257–266.
25 S. D. Ittel, *J. Organomet. Chem.*, 1980, **195**, 331–335.
26 John Emsley and D. Hall, *The Chemistry of Phosphorus*, Harper & Row Ltd, London, 1976.
27 a) SCALE3ABS, CrysAlisPro, Aglient Technologies Inc., Oxford, UK, 2015; b) G. M. Sheldrick, SADABS, Bruker AXS, Madison, USA, 2007.
28 a) R. C. Clark and J. S. Reid, *Acta Crystallogr. A*, 1995, **51**, 887–897; b) CrysAlisPro, Agilent Technologies Inc., Oxford, UK, 2015.
29 G. M. Sheldrick, *Acta Crystallogr. Sect. Found. Adv.*, 2015, **71**, 3–8.
30 G. M. Sheldrick, *Acta Crystallogr. A*, 2008, **64**, 112–122.
31 F. Neese, *Wiley Interdiscip. Rev. Comput. Mol. Sci.*, 2012, **2**, 73–78.
32 A. Schäfer, H. Horn and R. Ahlrichs, *J. Chem. Phys.*, 1992, **97**, 2571–2577.
33 A. D. Becke, *J. Chem. Phys.*, 1993, **98**, 5648–5652.
34 A. D. Becke, *J. Chem. Phys.*, 1993, **98**, 1372–1377.
35 F. Weigend and R. Ahlrichs, *Phys. Chem. Chem. Phys. PCCP*, 2005, **7**, 3297–3305.

36 C. Lee, W. Yang and R. G. Parr, *Phys. Rev. B*, 1988, **37**, 785–789.
37 A. D. Becke, *Phys. Rev. A*, 1988, **38**, 3098–3100.
38 J. P. Perdew, *Phys. Rev. B*, 1986, **33**, 8822–8824.
39 S. Grimme, S. Ehrlich and L. Goerigk, *J. Comput. Chem.*, 2011, **32**, 1456–1465.
40 S. Grimme, J. Antony, S. Ehrlich and H. Krieg, *J. Chem. Phys.*, 2010, **132**, 154104.
41 D. L. Dodds, M. F. Haddow, A. G. Orpen, P. G. Pringle and G. Woodward, *Organometallics*, 2006, **25**, 5937–5945.
42 R. A. Oliveira, R. O. Silva, G. A. Molander and P. H. Menezes, *Magn. Reson. Chem. MRC*, 2009, **47**, 873–878.

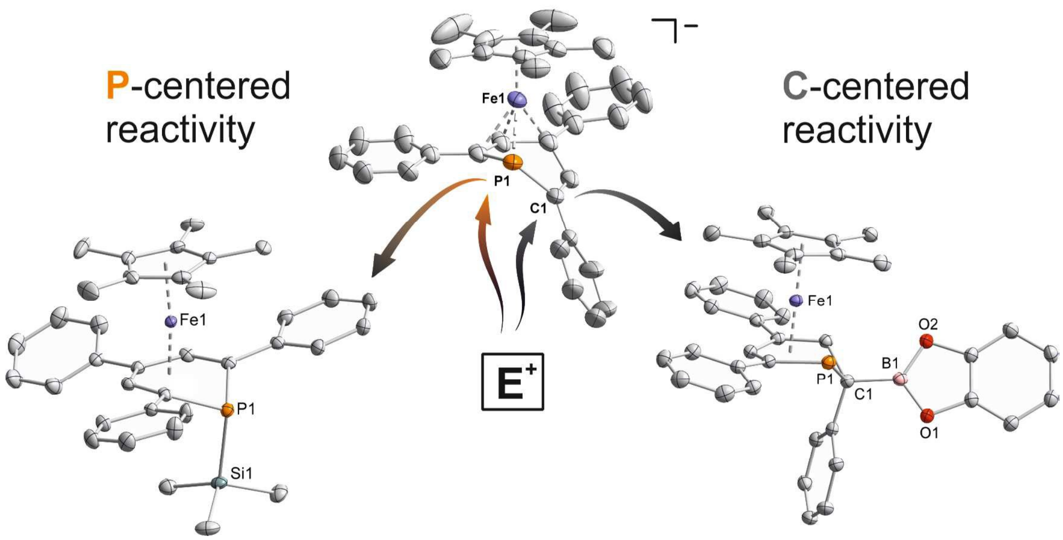

Electrophilic attack of π-coordinated 2,4,6-triphenylphosphinine afforded a range of novel complexes with substituted η^5-phosphacyclohexadienyl ligands.